Electronic Supplementary Material (ESI) for ChemComm.

Supporting Information

for

Rearrangement of an aniline linked perylene bisimide under acidic conditions and visible to near-infrared emission from intramolecular charge-transfer state of its fused derivatives

Mitsuru Kojima, Akira Tamoto, Naoki Aratani* and Hiroko Yamada*

Contents

1. Instrumentation and Materials

^{1}H NMR (400 MHz) and ^{13}C NMR (100 MHz and 150 MHz) spectra were recorded with JEOL JNM-ECX 400, JEOL JNM-ECP 400 and JEOL JNM-ECA 600 spectrometers at ambient temperature by using tetramethylsilane as an internal standard. The high-resolution MS were measured by a JEOL spiralTOF JMS-S3000 spectrometer using positive ion modes. X−ray crystallographic data were recorded at 90 K on a Bruker APEX II X-ray diffractometer equipped with a large area CCD detector by using graphite monochromated Mo-Kα radiation for **3** and at 100 K on a Rigaku R-AXIS RAPID/S using Mo-Kα radiation for **5**.

UV/Vis absorption spectra were measured with a JASCO UV/Vis/NIR spectrophotometer V-570. CV measurements were conducted in a solution of 0.1 M $TBAPF_6$ in dry dichloromethane with a scan rate of 100 mV/s at room temperature in an argon-filled cell. A glassy carbon electrode and a Pt wire were used as a working and a counter electrode, respectively. An Ag/Ag^{+} electrode was used as reference electrodes, which were normalized with the half-wave potential of ferrocene/ferrocenium^{+} (Fc/Fc^{+}) redox couple.

TLC and gravity column chromatography were performed on Art. 5554 (Merck KGaA) plates and silica gel 60N (Kanto Chemical), respectively. All other solvents and chemicals were reagent-grade quality, obtained commercially, and used without further purification. For spectral measurements, spectral-grade solvents were purchased from Nacalai Tesque.

All DFT calculations were performed with a Gaussian 09 program package.[S1] The geometries were fully optimized at the Becke's three-parameter hybrid functional combined with the Lee-Yang-Parr correlation functional abbreviated as the B3LYP level of density functional theory. The 6-31G(d) bases set implemented was used for structure optimizations and frequency analyses.

2. Experimental Section

***N*,*N*'-Bis(2,6-diisopropylphenyl)-1,7-bis(*N*,*N*'-dimethylanilin-4-yl)-perylene-3,4,9,10-tetracarboxylic acid bisimide (1)**: A mixture of *N*,*N*'-(2,6-diisopropylphenyl)-1,7-dibromoperylene-3,4,9,10-tetracarboxilic acid bisimide (520 mg, 0.60 mmol), *N*,*N*'-dimethyl-4-(1,3,2-dioxaborolan-2-yl) aniline (1.2 g, 4.8 mmol), K_2CO_3 (190 mg, 1.8 mmol), and toluene (2.0 mL) was degassed by freeze-pump-thaw cycle for 3 times. Then, $PdCl_2$(dppf) (17 mg, 2.5 mol%, 0.015 mmol) was added under Ar flow and stirred for 24 h at 80°C. After cooling to room temperature, the reaction mixture was extracted with CH_2Cl_2. The organic layer was washed with brine and dried over Na_2SO_4. The mixture was concentrated in vacuo and purified by a flash silica gel column chromatography eluted with $CHCl_3$ and recrystallized from $CHCl_3$ / methanol to give pure compound **1** (228 mg, 0.24 mmol) as a green solid in 40% yield. ^{1}H NMR ($CDCl_3$, 400 MHz, ppm) δ 1.16 (d, J = 6.4 Hz, 24H), 2.76 (sep, 4H), 3.08 (s, 12H), 6.79 (d, J = 10.5 Hz, 4H), 7.33 (d, J = 8.2 Hz, 4H), 7.45−7.53 (m, 6H), 8.13 (d, J = 9.0 Hz, 2H), 8.21 (d, J = 9.0 Hz, 2H) and 8.71 (s, 2H). ^{13}C NMR ($CDCl_3$, 100 MHz, ppm) δ 24.05, 29.09, 40.32, 113.40, 121.32, 121.91, 123.98, 124.11, 128.08 129.36, 130.05, 130.21, 130.67, 132.61, 136.10, 136.26, 141.61, 142.88, 145.61, 150.44, and 163.74. HR-MS (MALDI): Calcd: 948.46091, Obs. [M^+]: 948.46145. UV-vis (CH_2Cl_2): λ_{max} (ε [M^{-1} cm^{-1}]) = 314 (4.4×10^4), 488 (3.1×10^4) and 683 (1.4×10^4) nm.

***N*,*N*'-Bis(2,6-diisopropylphenyl)-4,12-bis(dimethylamino)benzo[*a*,*j*]coronene-1,8,9,16-tetracarboxylic acid bisimide (2) and *N*,*N*'-bis(2,6-diisopropylphenyl)-4,13-bis(dimethylamino)-benzo[*a*,*j*]coronene-1,8,9,16-tetracarboxylic acid bisimide (3):** To a mixture of **1** (100 mg, 0.10 mmol) and 2,3-dichloro-5,6-dicyanobenzoquinone (DDQ) (60 mg, 0.50 mmol), *o*-dichlorobenzene (50 mL) was added and degassed by argon for 20 min. TfOH (0.10 mL) was added and the mixture was stirred for 30 min at 150°C. After cooling to room temperature, the reaction mixture was neutralized by triethylamine, and was extracted with CH_2Cl_2. The organic layer was washed with water, brine, and dried over Na_2SO_4. The mixture of **2** and **3** was concentrated and purified by a flash silica gel column chromatography with CH_2Cl_2 in 14.4% and 16.6% yield, respectively (determined from ^{1}H NMR). Then, **2** and **3** were further purified by three times of a flash silica gel column chromatography with a 1:3 mixture of ethyl acetate and *n*-hexane to give pure compounds **2** (0.5 mg, 0.001 mmol) and **3** (1 mg, 0.002 mmol) as a dark green solid. ^{1}H NMR ($CDCl_3$, 400 MHz, ppm) **2**; δ 1.27 (d, J = 4.4 Hz, 24H), 3.01 (sep, 4H), 3.40 (s, 12H), 7.45 (d, J = 6.0 Hz, 4H), 7.58 (t, J = 6.0 Hz, 2H), 7.68 (d, J = 5.0 Hz, 2H), 8.52 (s, 2H), 9.39 (d, J = 6.2 Hz, 2H), and 10.53 (s, 2H); HR-MS (MALDI): Calcd: 944.42961, Obs. [M^+]: 944.42999. UV-vis (CH_2Cl_2): λ_{max} (ε [M^{-1} cm^{-1}]) = 326 (4.6×10^4), 400 (3.9×10^4) 460 (1.0×10^4), 491 (2.2×10^4) and 644 (1.1×10^4) nm; **3**; δ 1.26–1.30 (m, 24H), 2.96–3.06 (m, 4H), 3.40 (s, 12H), 7.45 (d, J = 6.0 Hz, 4H), 7.59 (t, J = 6.0 Hz, 2H), 7.68 (d, J = 5.0 Hz, 2H), 8.53 (s, 2H), 9.39 (d, J = 6.2 Hz, 2H), 10.41 (s, 2H), and 10.67 (s, 2H); HR-MS (MALDI): Calcd: 944.42961, Obs. [M^+]: 944.43003. λ_{max} (ε [M^{-1} cm^{-1}]) = 324 (4.4×10^4), 377 (4.7×10^4), 418 (1.6×10^4), 447 (2.3×10^4) and 601 (1.6×10^4) nm.

***N*,*N*'-Bis(2,6-diisopropylphenyl)-1,7-bis(10*H*-phenothiazine-3-yl)-perylene-3,4,9,10-tetracarboxylic acid bisimide (4):** A mixture of *N*,*N*'-(2,6-diisopropylphenyl)-1,7-dibromoperylene-3,4,9,10-tetracarboxylic acid bisimide (138 mg, 0.144 mmol), 3-bromo-10*H*-phenothiazine (80 mg, 0.288 mmol), K_2CO_3 (200 mg, 1.44 mmol), TBABr (5 mg, 0.0144 mmol), toluene (2.5 mL), and water (2.5 mL), was degassed by freeze-pump-thaw for 3 timers. Then, $PdCl_2$(dppf) (12 mg, 0.0144 mmol) was added under Ar flow and stirred for 3 h at 90°C. After cooling to room temperature, the reaction mixture was extracted with CH_2Cl_2. The organic layer was washed with brine and dried over Na_2SO_4. The mixture was concentrated in *vacuo* and purified by a flash silica gel column chromatography eluted with CH_2Cl_2 and recrystallized from CH_2Cl_2 / methanol to give pure compound **4** (64 mg, 0.24 mmol) as a green solid in 40% yield. ^{1}H NMR ($CDCl_3$, 400 MHz, ppm) δ 1.13–1.20 (m, 24H), 2.76 (sep, 4H), 6.16 (s, 2H), 6.49 (d, J = 7.8 Hz, 2H), 6.60–6.70 (m, 2H), 6.84 (t, J = 7.8 Hz, 2H), 6.92–7.04 (m, 4H), 7.34 (d, J = 8.7 Hz, 4H), 7.49 (t, J = 8.7 Hz, 2H), 8.19 (d, J = 8.7 Hz, 2H), 8.31 (d, J = 8.7 Hz, 2H) and 8.65 (s, 2H); HR-MS (MALDI): Calcd: 1104.37375, Obs. [M^+]: 1104.37295. UV-vis (CH_2Cl_2): λ_{max} (ε [M^{-1} cm^{-1}]) = 513 (2.2×10^4) and 620 (0.8×10^4) nm.

Phenothiazine-fused PBI 5: To a mixture of **4** (120 mg, 0.11 mmol) and DDQ (126 mg, 0.55 mmol), *o*-dichlorobenzene (20 mL) was added and degassed by argon for 20 min. TfOH (0.10 mL) was added and stirred for 90 min at 120°C. After cooling to room temperature, the reaction mixture was neutralized by triethylamine, and it was extracted with CH_2Cl_2. The organic layer was washed with water, brine, and dried over Na_2SO_4. The mixture was concentrated in *vacuo* and purified by a flash silica gel column chromatography eluted with CH_2Cl_2 and recrystallized from CH_2Cl_2 / methanol to give pure compound **5** (14 mg, 0.013 mmol) as a dark green solid in 12% yield. ^{1}H NMR ($CDCl_3$, 400 MHz, ppm) δ 1.21–1.32 (m, 24H), 2.99 (sep, 4H), 6.58 (s, 2H), 6.69 (d, J = 8.0 Hz, 2H), 6.90 (t, J = 7.6 Hz, 2H), 7.04–7.11 (m, 2H), 7.47 (d, J = 7.4 Hz, 4H), 7.61 (t, J = 7.4 Hz, 2H), 8.44 (s, 2H), 9.02 (s, 2H), 10.36 (s, 2H) and 10.40 (s, 2H), HR-MS (MALDI): Calcd: 1100.34245, Obs. [M^+]: 1100.34202. UV-vis (CH_2Cl_2): λ_{max} = 353, 391, 410, 478, 511, 623 nm.

3. NMR Spectra

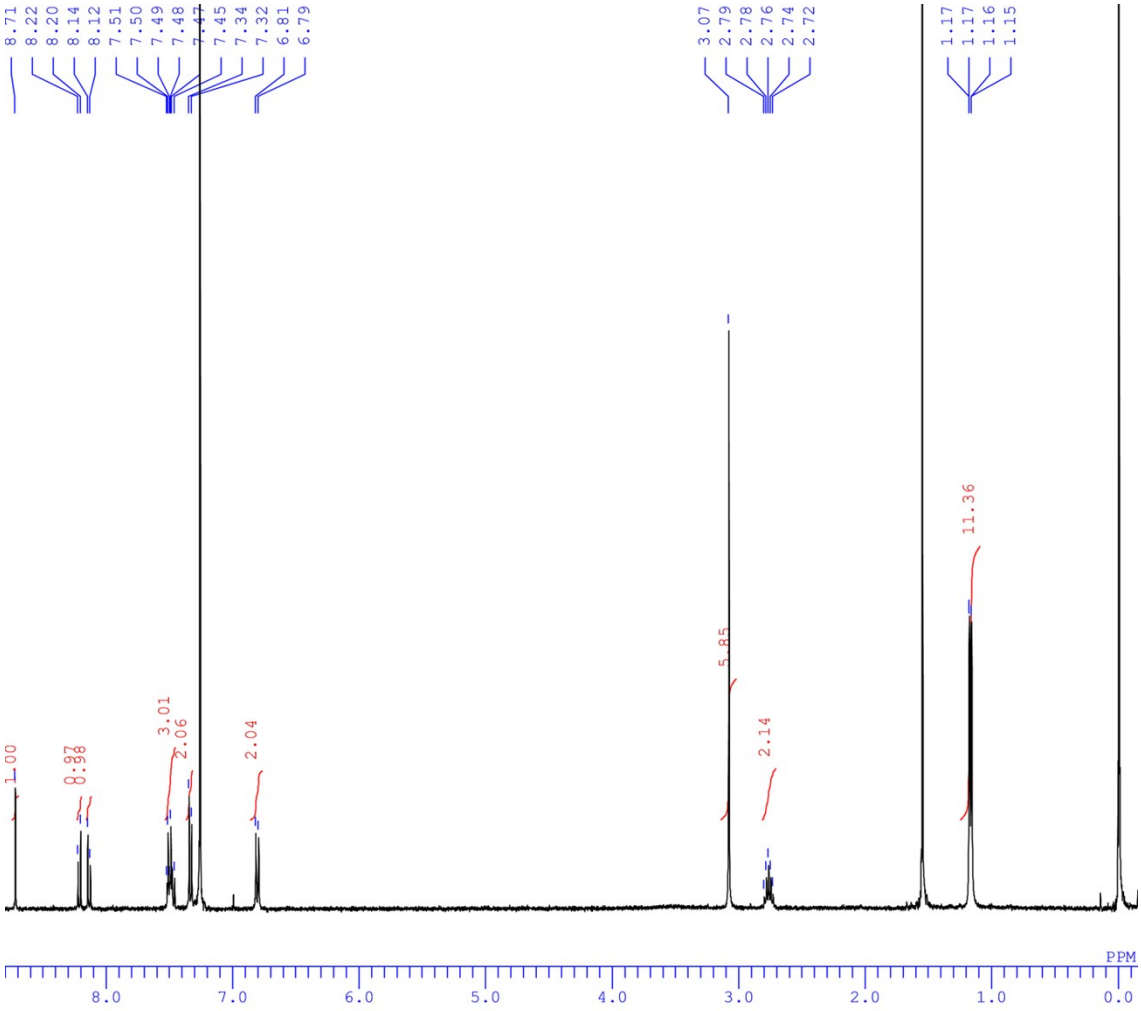

Figure S1. ^{1}H NMR spectrum of **1** in $CDCl_3$.

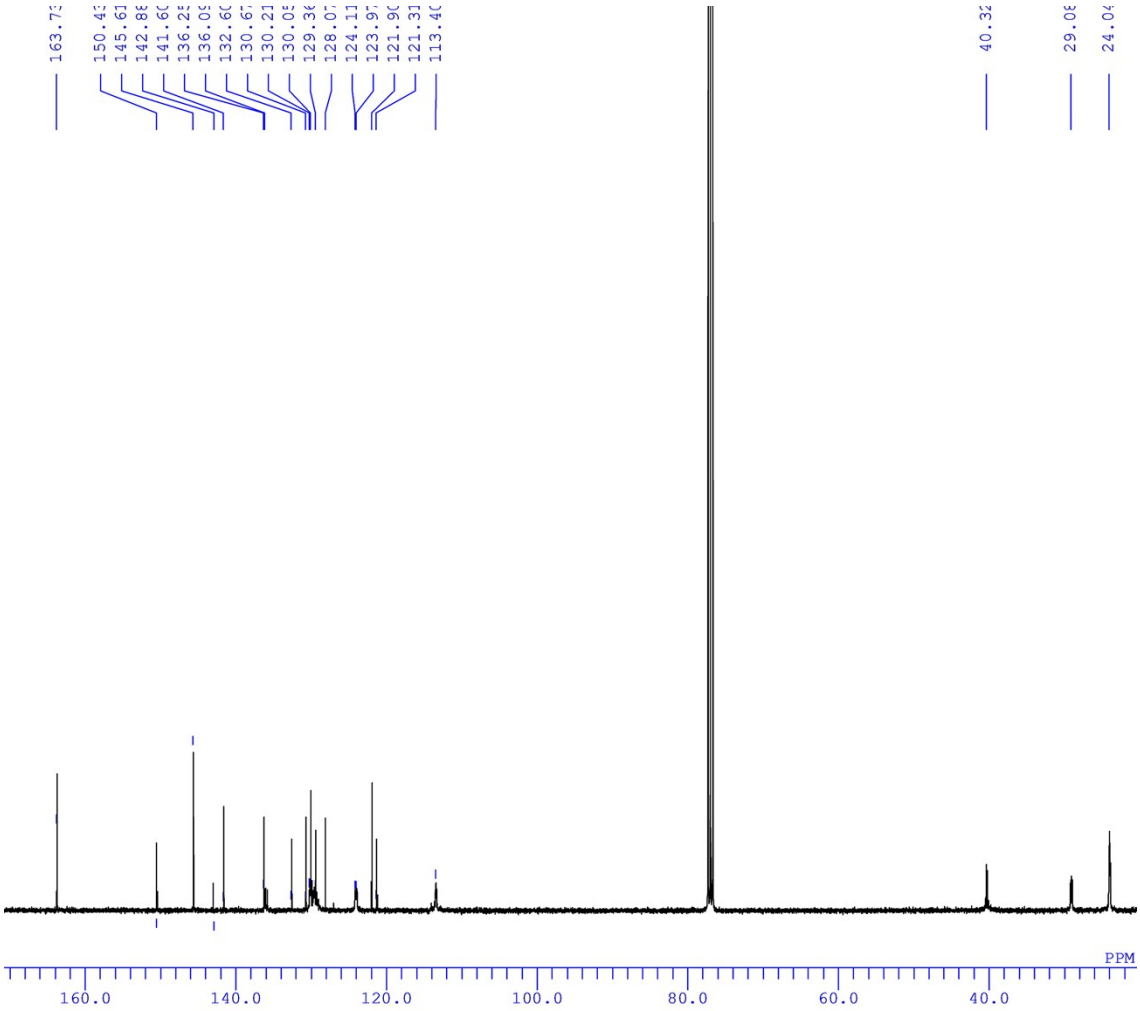

Figure S2. ^{13}C NMR spectrum of **1** in $CDCl_3$.

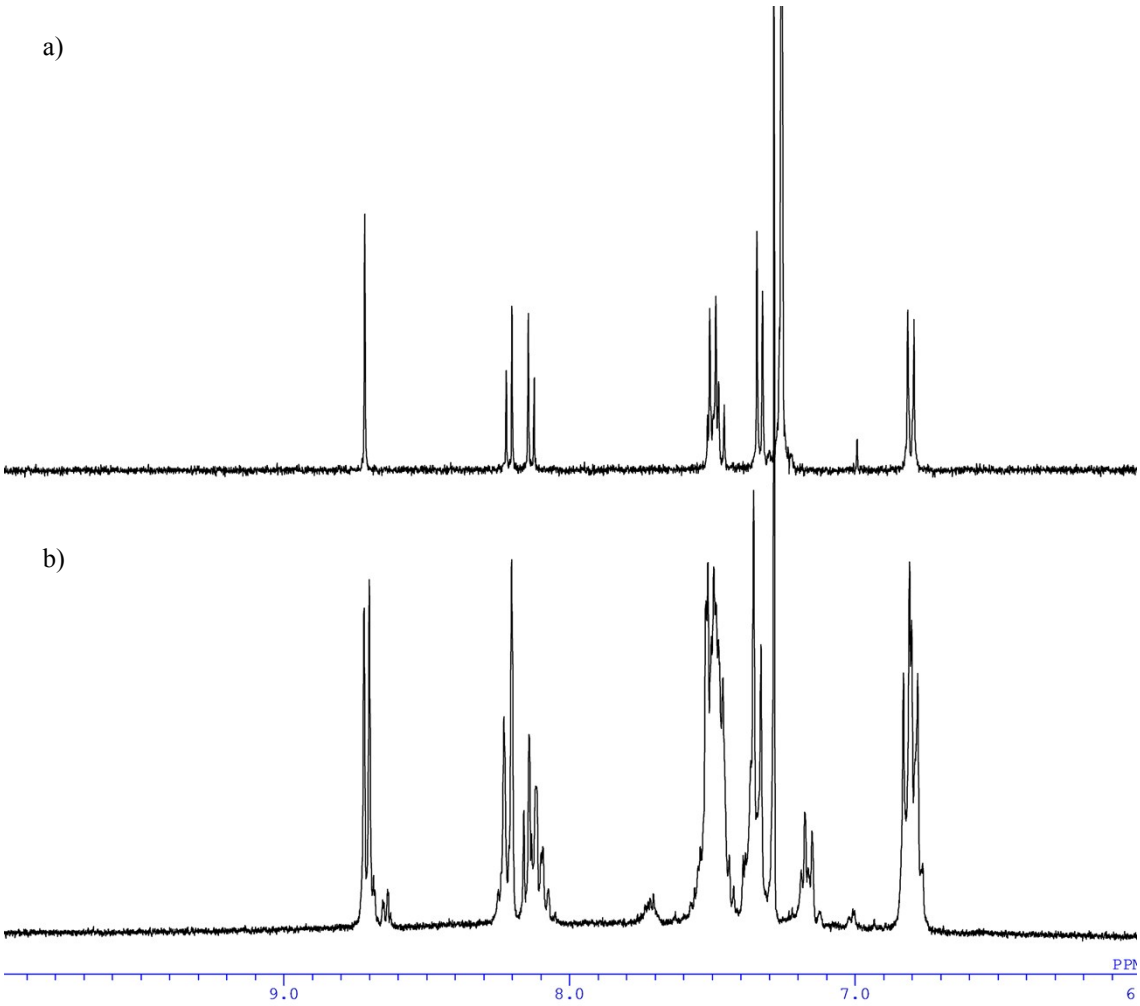

Figure S3. ^{1}H NMR spectra of a) pure **1** and b) the products after heating with acid in $CDCl_3$.

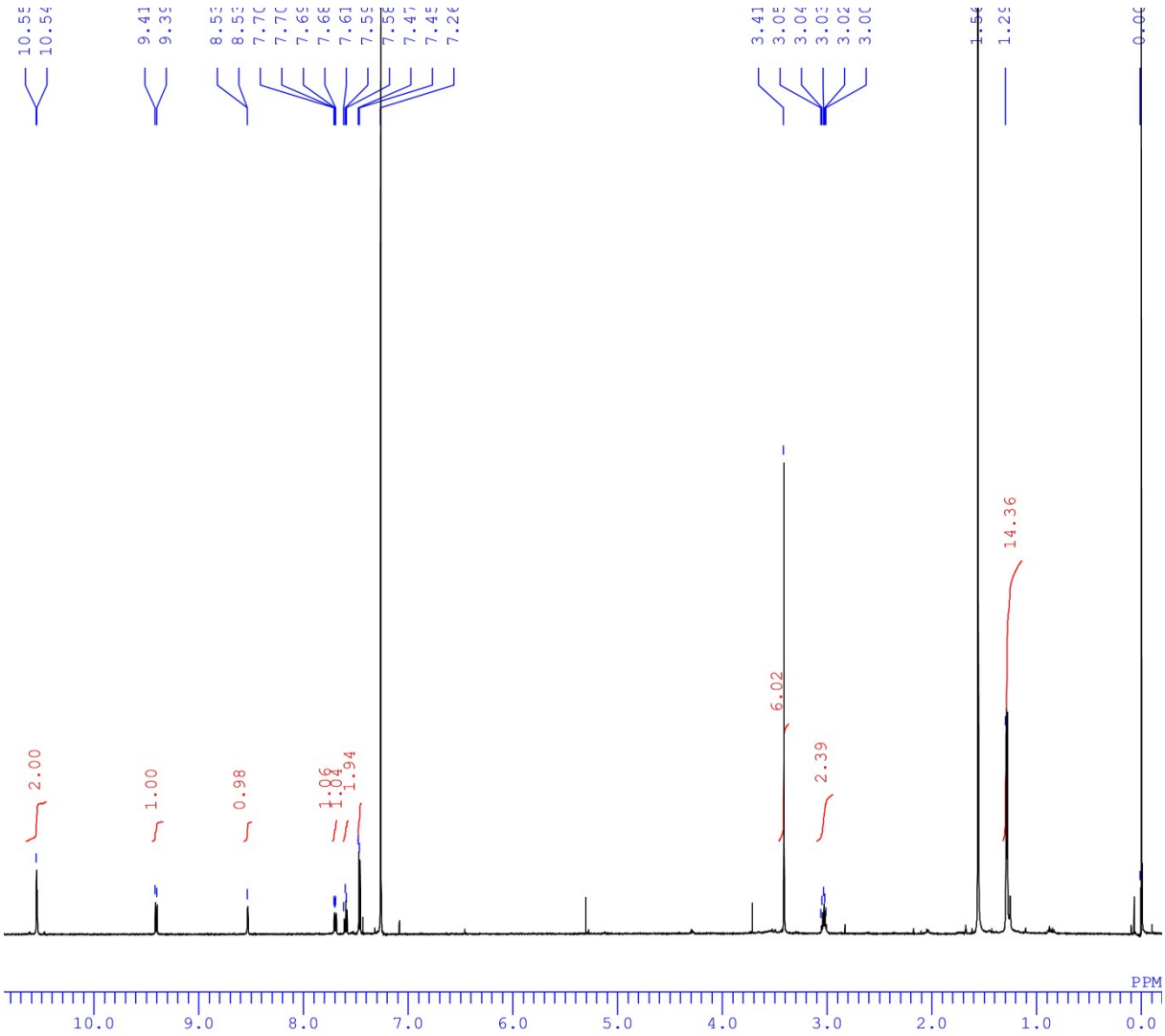

Figure S4. ^{1}H NMR spectrum of **2** in $CDCl_3$.

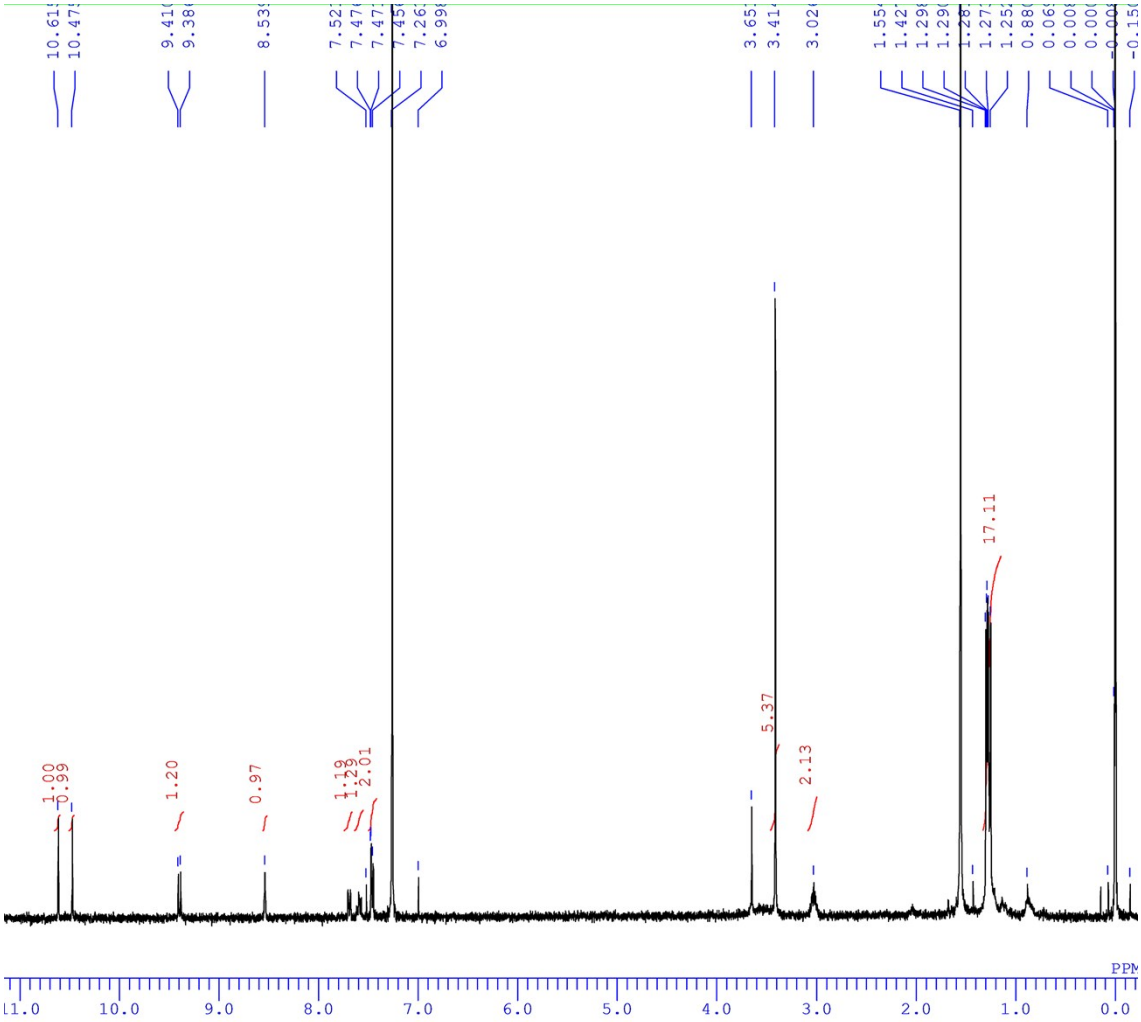

Figure S5. ^{1}H NMR spectrum of **3** in $CDCl_3$.

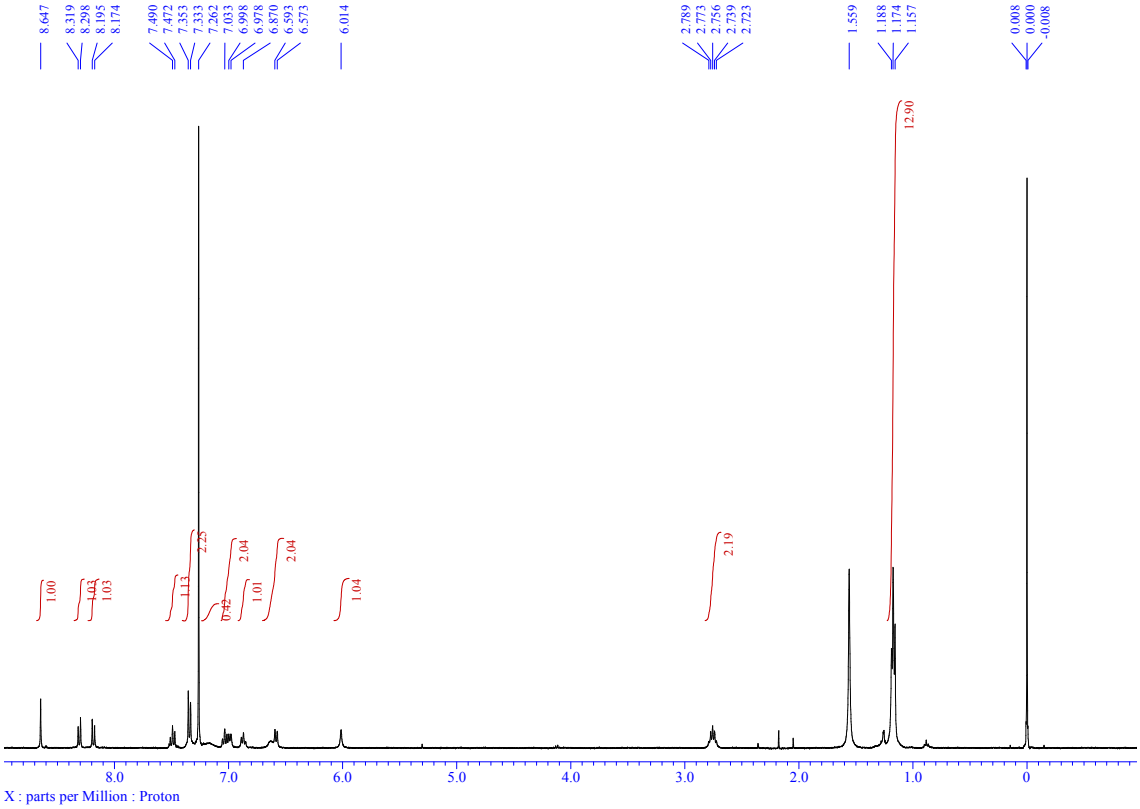

Figure S6. ^{1}H NMR spectrum of **4** in $CDCl_3$.

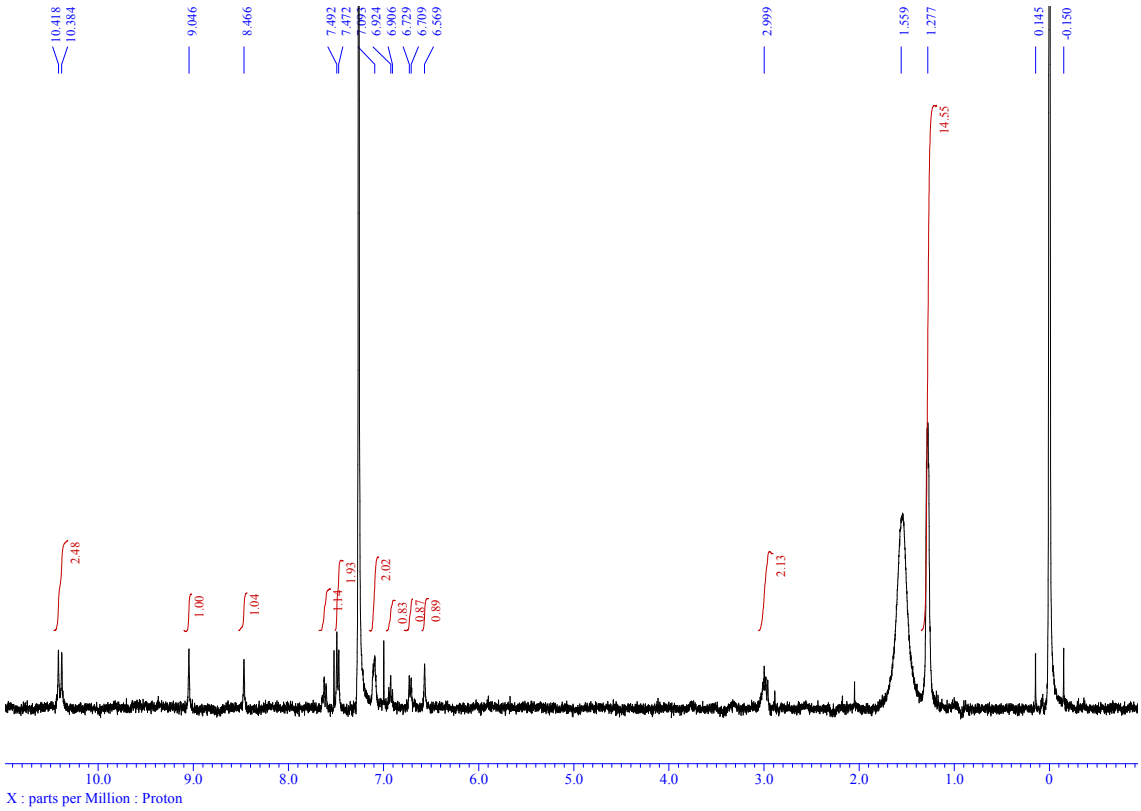

Figure S7. ^{1}H NMR spectrum of **5** in $CDCl_3$

4. HR-MS

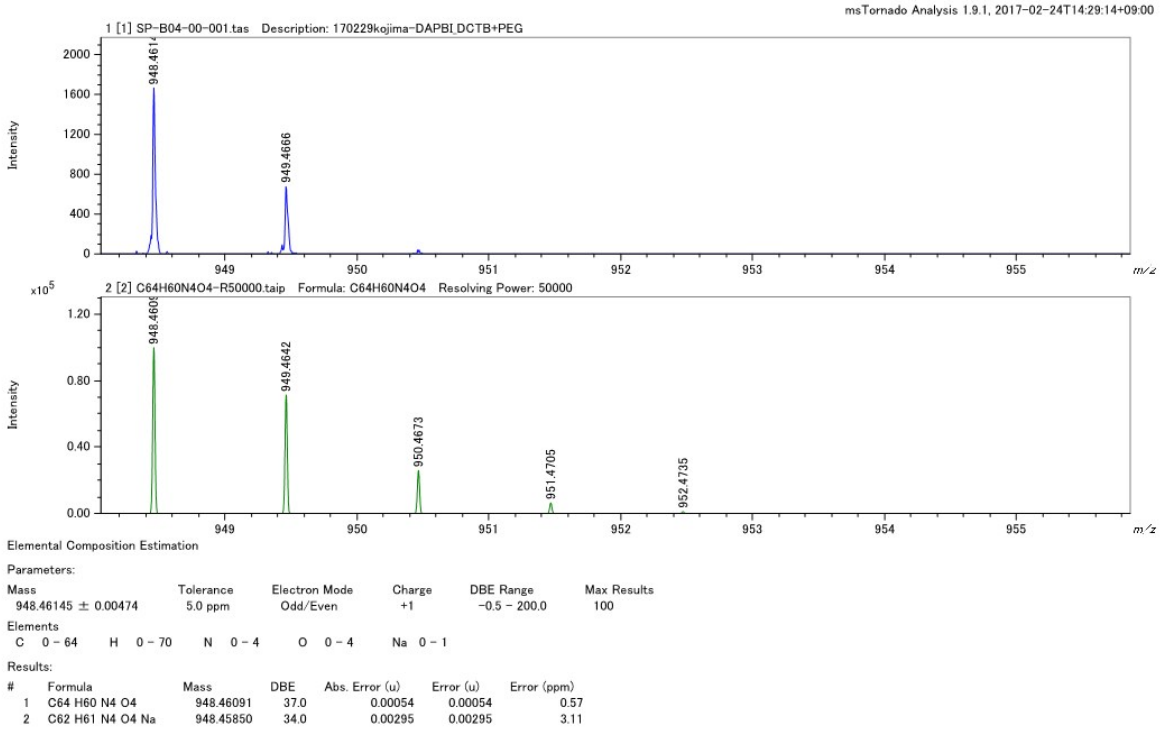

Figure S8. HR-Spiral-MALDI-TOF mass spectrum of **1**.

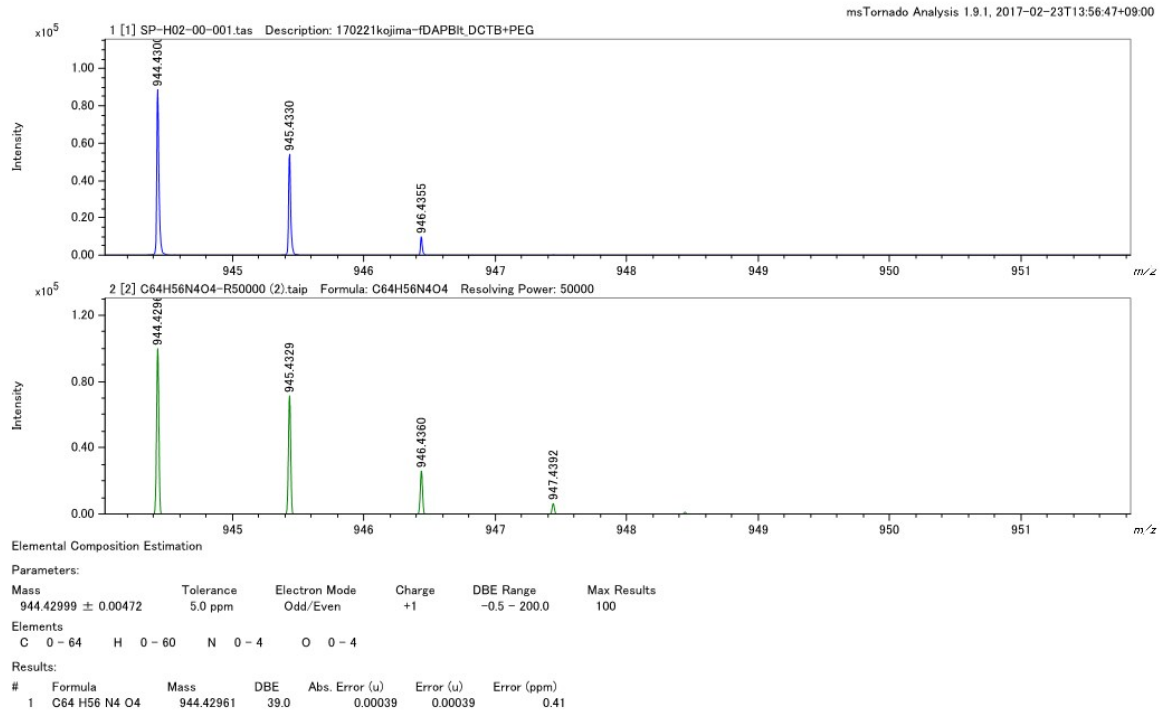

Figure S9. HR-Spiral-MALDI-TOF mass spectrum of **2**.

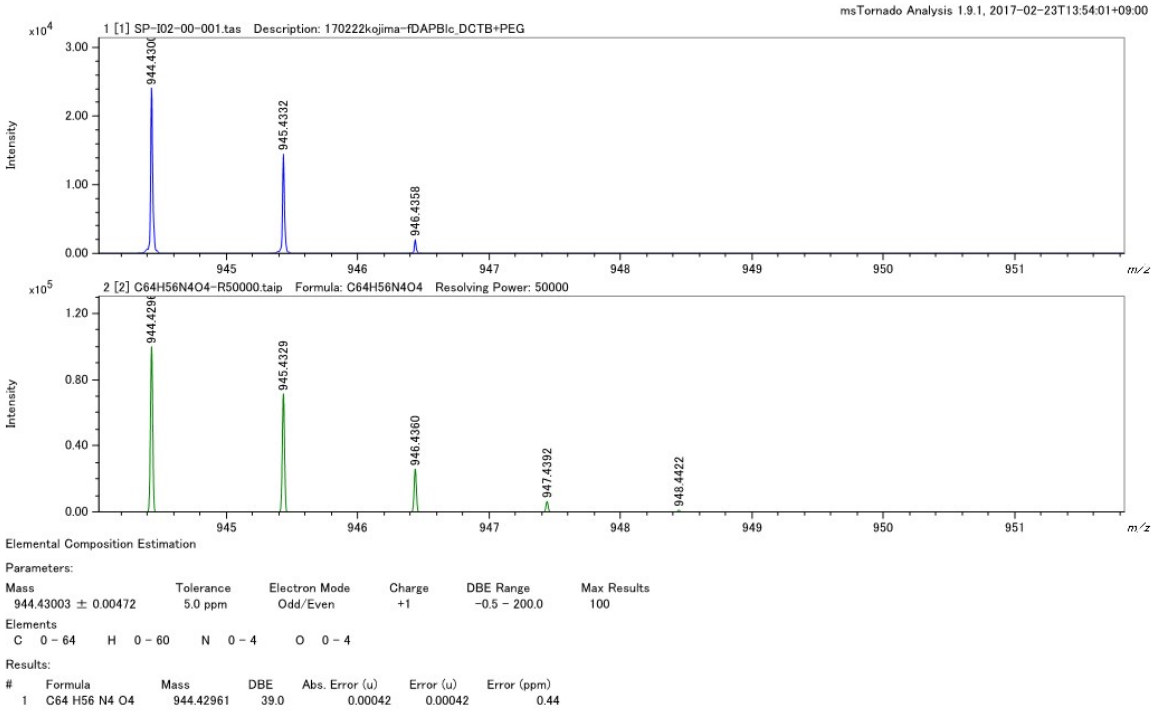

Figure S10. HR-Spiral-MALDI-TOF mass spectrum of **3**.

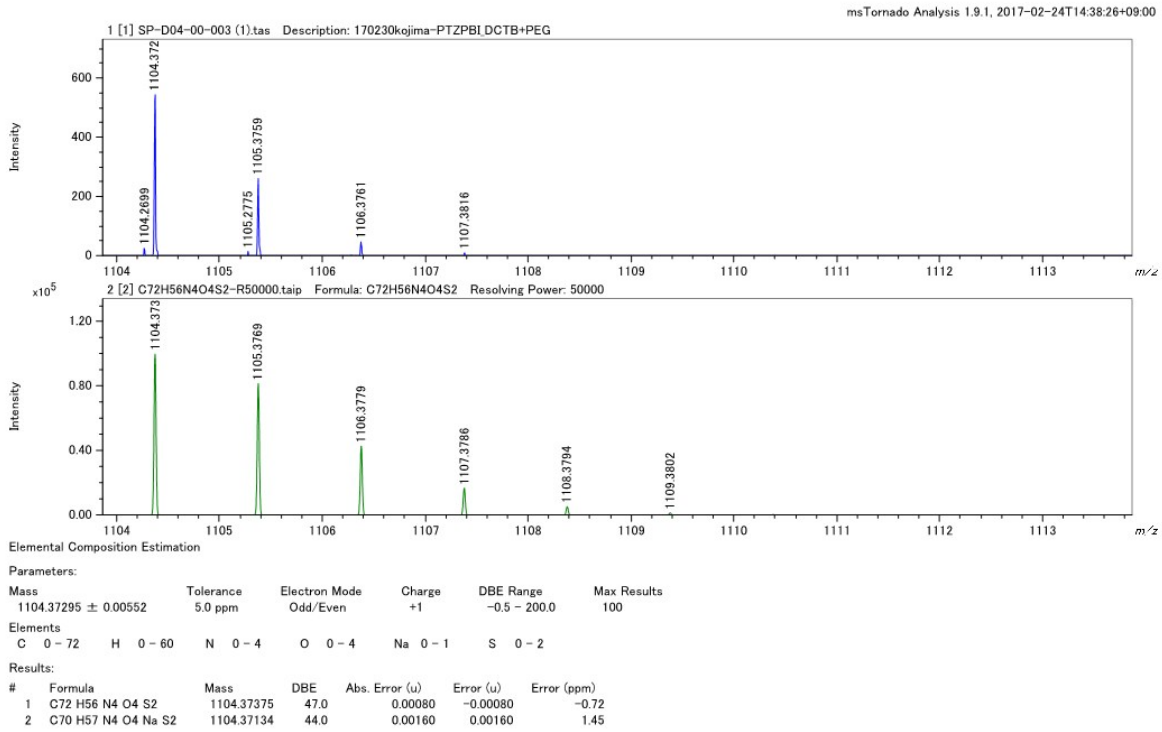

Figure S11. Spiral-MALDI-TOF mass spectrum of **4**.

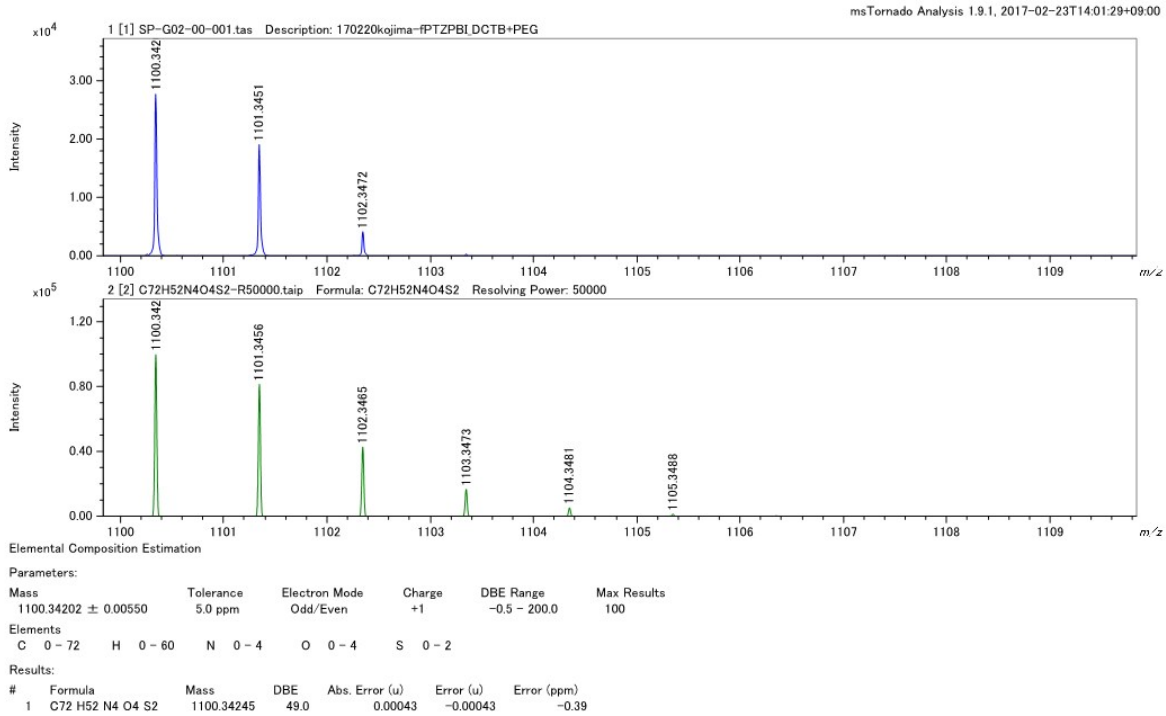

Figure S12. Spiral-MALDI-TOF mass spectrum of **5**.

5. UV-vis-NIR Absorption and Fluorescence Spectra

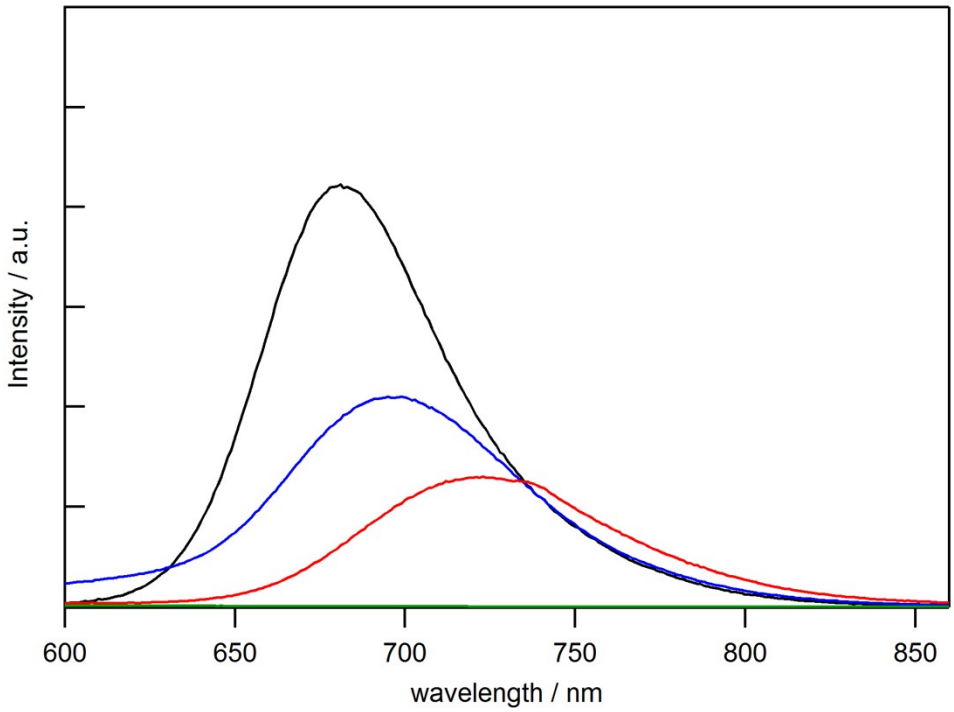

Figure S13. Fluorescence spectra of **3** in toluene (black), $CHCl_3$ (blue), CH_2Cl_2 (red), and DMF (green).

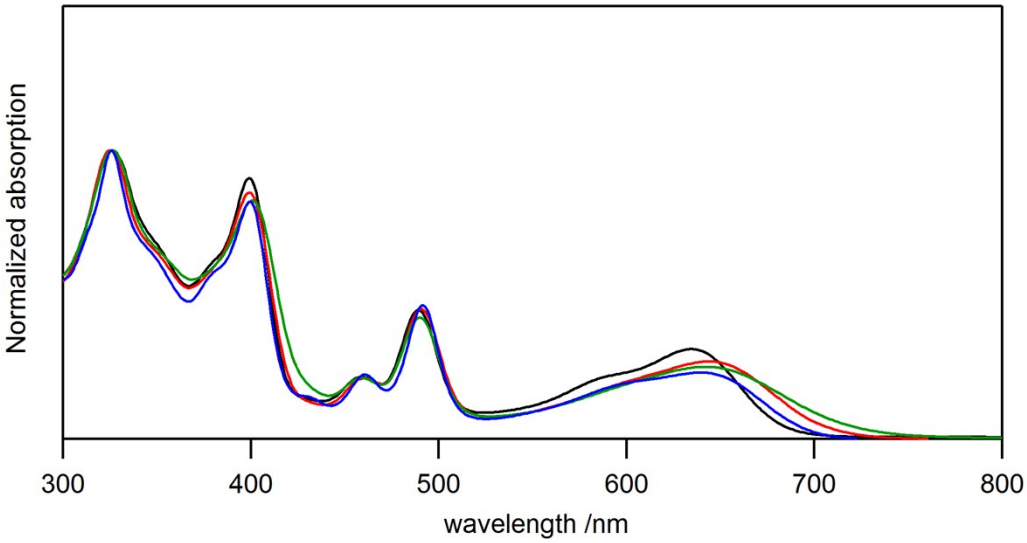

Figure S14. Normalized UV-vis absorption spectra of **2** in toluene (black), $CHCl_3$ (blue), CH_2Cl_2 (red), and DMF (green).

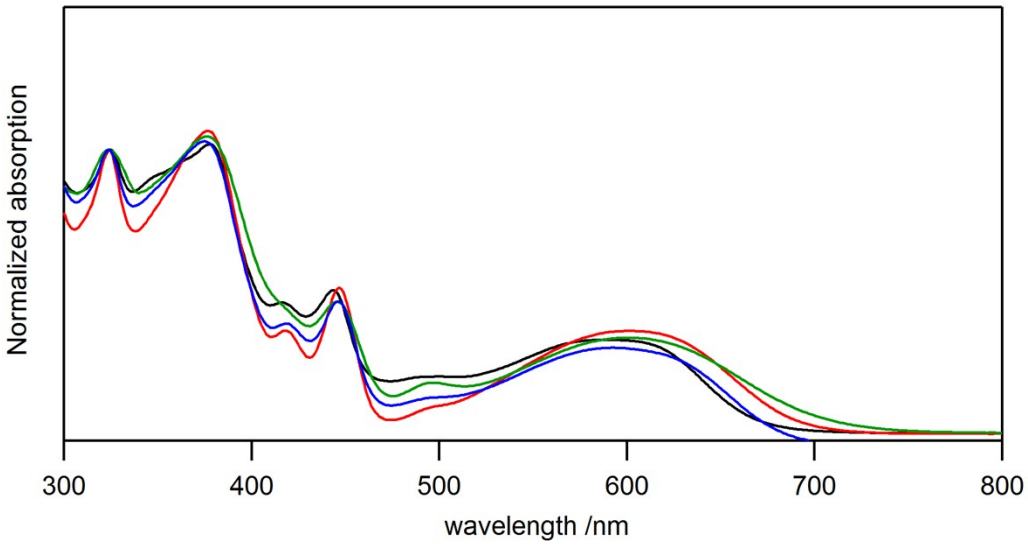

Figure S15. Normalized UV-vis absorption spectra of **3** in toluene (black), $CHCl_3$ (blue), CH_2Cl_2 (red), and DMF (green).

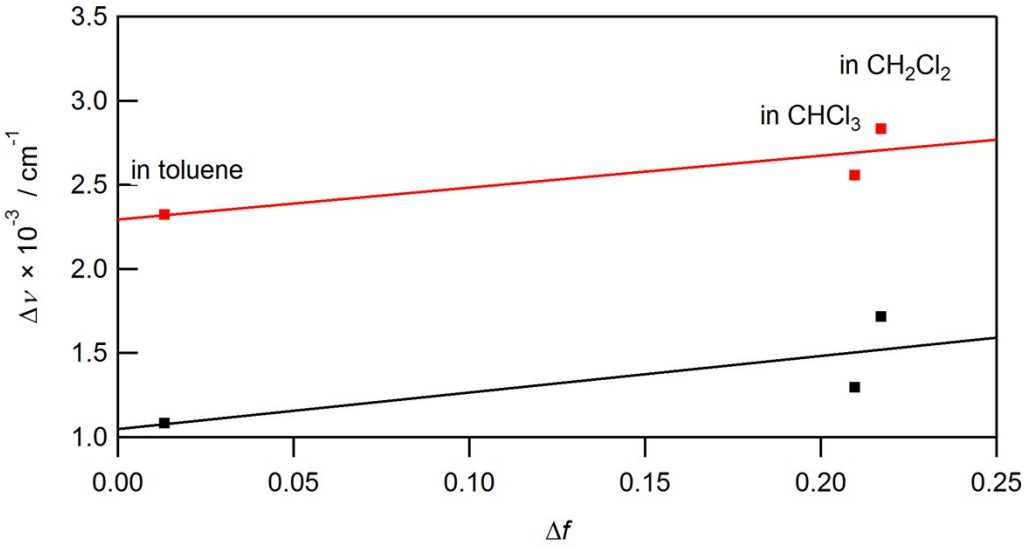

Figure S16.Lippert-Mataga plots of **2** (black) and **3** (red).

6. Molecular Orbital

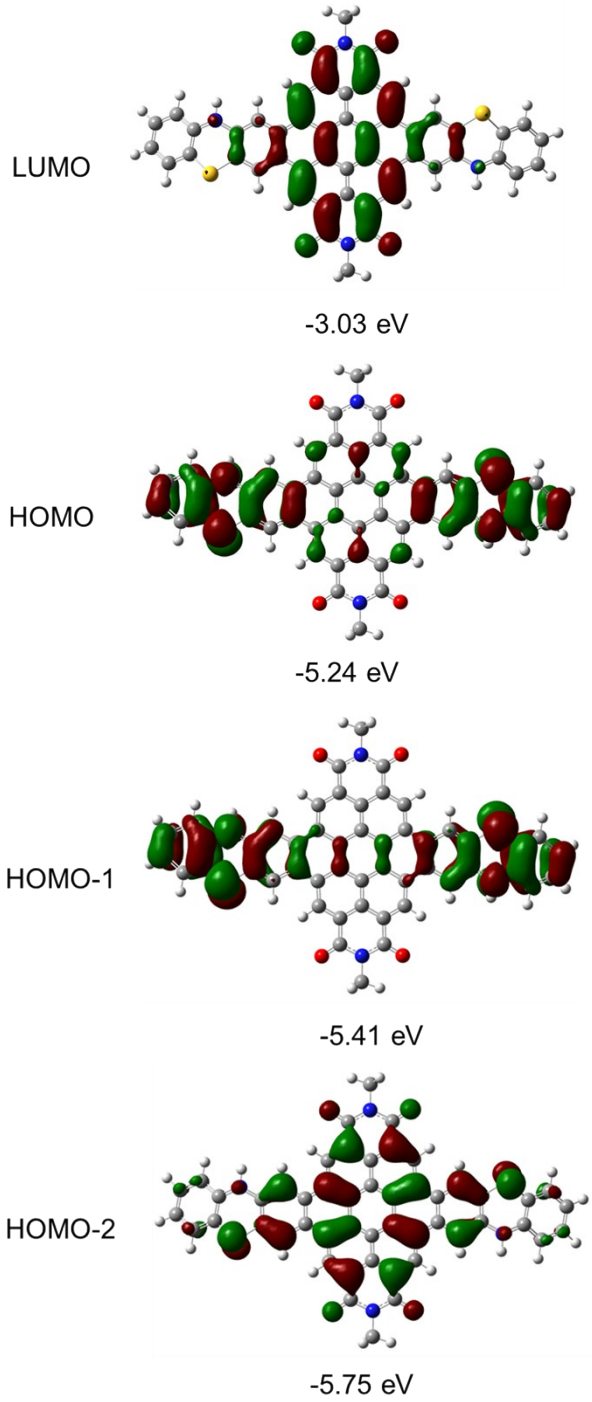

Figure S17. MO diagram of **5'** based on the calculations at the B3LYP/6-31G* level.

7. X-Ray Crystal Data

Table S1. Crystal data and structure refinement for **3**

Empirical formula	$C_{64}H_{56}N_4O_4$
Formula weight	945.12
Temperature	90 K
Wavelength	0.71073 Å
Crystal system	Monoclinic
Space group	$P2_1$
Unit cell dimensions	a = 10.9335(9) Å
	b = 13.6371(12) Å β = 98.801(2)°
	c = 22.866(2) Å
Volume	3369.2(5) Å^3
Z	2
Density (calculated)	0.932 g/cm^3
Absorption coefficient	0.058 mm^{-1}
F(000)	1000
Crystal size	0.500 x 0.300 x 0.300 mm^3
Theta range for data collection	1.744 to 26.000°
Index ranges	$-13 \le h \le 12$, $-16 \le k \le 16$, $-17 \le l \le 28$
Reflections collected	19412
Independent reflections	12991 [R(int) = 0.0266]
Completeness to theta = 25.242°	99.4%
Absorption correction	Semi-empirical from equivalents
Max. and min. transmission	0.983 and 0.852
Refinement method	Full-matrix least-squares on F^2
Data / restraints / parameters	12991 / 45 / 730
Goodness-of-fit on F^2	0.940
Final R indices [$I > 2\sigma(I)$]	R_1 = 0.0797, wR_2 = 0.2100
R indices (all data)	R_1 = 0.1190, wR_2 = 0.2357
Absolute structure parameter	0(3)
Largest diff. peak and hole	0.686 and –0.267 e.Å^{-3}

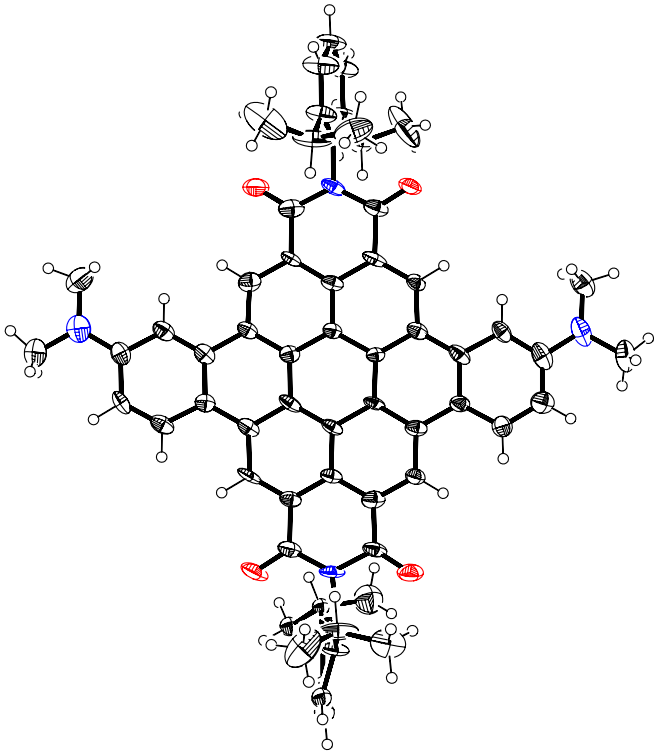

Figure S18. X-ray crystal structure of **3**. Thermal ellipsoids were scaled to 50% probability.

Table S2. Crystal data and structure refinement for **5**

Empirical formula	$C_{72}H_{52}N_4O_4S_2$	
Formula weight	1101.29	
Temperature	103(2) K	
Wavelength	0.71075 Å	
Crystal system	Triclinic	
Space group	*P*-1	
Unit cell dimensions	a = 10.5479(11) Å	α = 82.196(6)°
	b = 12.3384(13) Å	β = 72.123(5)°
	c = 16.2391(17) Å	γ = 64.915(5)°
Volume	1821.6(3) Å^3	
Z	1	
Density (calculated)	1.004 g/cm^3	
Absorption coefficient	0.117 mm^{-1}	
F(000)	576	
Crystal size	0.150 x 0.040 x 0.020 mm^3	
Theta range for data collection	3.195 to 23.500°	
Index ranges	$-11 \le h \le 11$, $-13 \le k \le 13$, $-18 \le l \le 18$	
Reflections collected	20855	
Independent reflections	5349 [R(int) = 0.1433]	
Completeness to theta = 23.500°	99.4%	
Absorption correction	Semi-empirical from equivalents	
Max. and min. transmission	0.9140 and 0.3370	
Refinement method	Full-matrix least-squares on F^2	
Data / restraints / parameters	5349 / 29 / 395	
Goodness-of-fit on F^2	1.001	
Final R indices [$I > 2\sigma(I)$]	R_1 = 0.0911, wR_2 = 0.1591	
R indices (all data)	R_1 = 0.2158, wR_2 = 0.1938	
Largest diff. peak and hole	0.259 and –0.179 e.Å^{-3}	

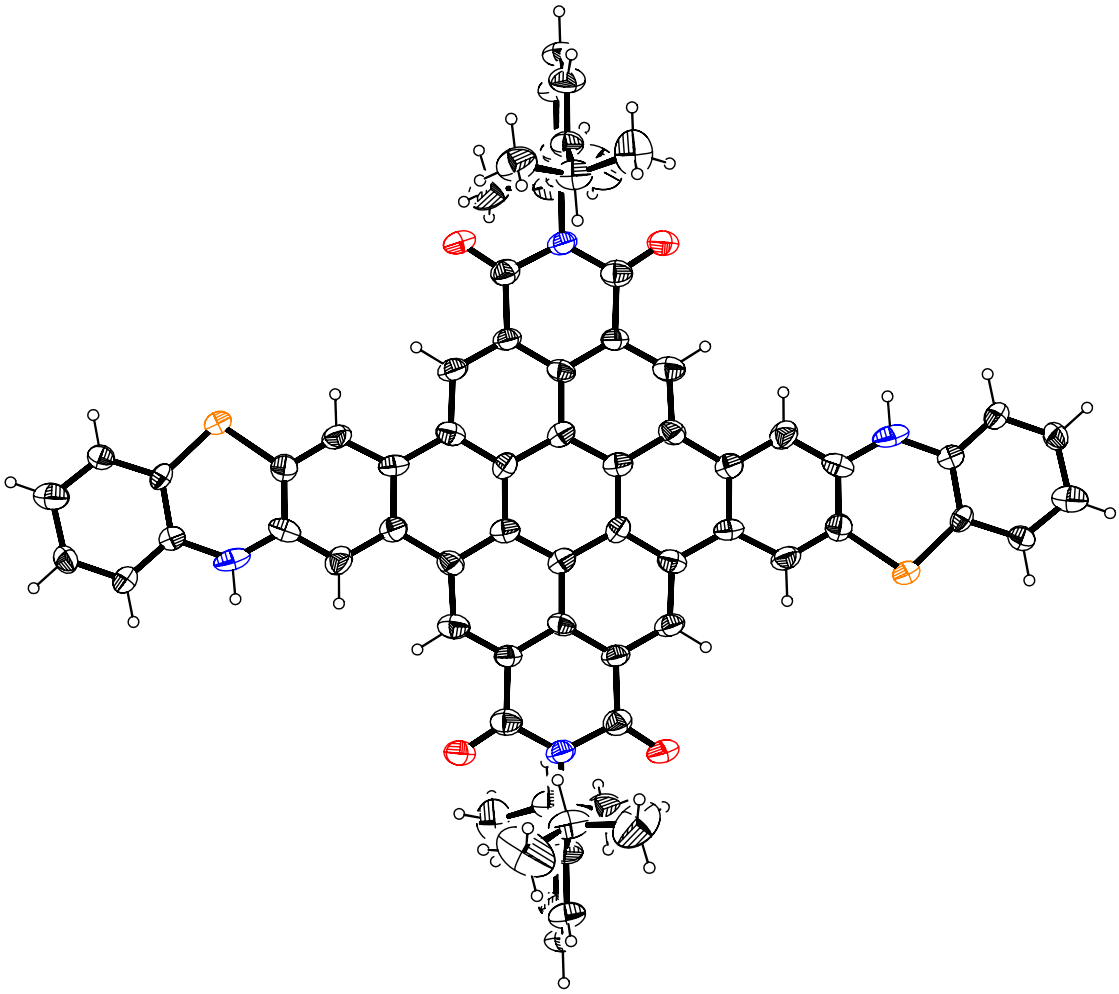

Figure S19. X-ray crystal structure of **5**. Thermal ellipsoids were scaled to 30% probability.

8. References

[S1] Gaussian 09, Revision A.02, M. J. Frisch, G. W. Trucks, H. B. Schlegel, G. E. Scuseria, M. A. Robb, J. R. Cheeseman, G. Scalmani, V. Barone, B. Mennucci, G. A. Petersson, H. Nakatsuji, M. Caricato, X. Li, H. P. Hratchian, A. F. Izmaylov, J. Bloino, G. Zheng, J. L. Sonnenberg, M. Hada, M. Ehara, K. Toyota, R. Fukuda, J. Hasegawa, M. Ishida, T. Nakajima, Y. Honda, O. Kitao, H. Nakai, T. Vreven, J. A. Montgomery, Jr., J. E. Peralta, F. Ogliaro, M. Bearpark, J. J. Heyd, E. Brothers, K. N. Kudin, V. N. Staroverov, R. Kobayashi, J. Normand, K. Raghavachari, A. Rendell, J. C. Burant, S. S. Iyengar, J. Tomasi, M. Cossi, N. Rega, J. M. Millam, M. Klene, J. E. Knox, J. B. Cross, V. Bakken, C. Adamo, J. Jaramillo, R. Gomperts, R. E. Stratmann, O. Yazyev, A. J. Austin, R. Cammi, C. Pomelli, J. W. Ochterski, R. L. Martin, K. Morokuma, V. G. Zakrzewski, G. A. Voth, P. Salvador, J. J. Dannenberg, S. Dapprich, A. D. Daniels, O. Farkas, J. B. Foresman, J. V. Ortiz, J. Cioslowski, and D. J. Fox, Gaussian, Inc., Wallingford CT, 2009.